

Numerical Modeling of Vibrational Nonequilibrium Detonations in Hydrogen-Oxygen Mixtures

S Mohamed Hussain, Anil S. Karthik, Ashlesh Dahake, Ranjay K. Singh, Ajay V. Singh*

Department of Aerospace Engineering, Indian Institute of Technology Kanpur,
Kanpur-208016, India

1 Introduction

Detonation waves in hydrogen-oxygen mixtures play a crucial role in high-energy propulsion systems. Computational modeling of these detonation waves has been an extensive area of research over the past few decades. With the growth in computational power, the development of reduced reaction mechanisms, and algorithmic advancements such as adaptive mesh refinement, the dynamics of complex detonation waves can now be modeled with enhanced accuracy and effectiveness. Despite significant advancements, many challenges remain in accurately capturing the effects of thermodynamic and chemical interactions, particularly vibrational nonequilibrium, which is ignored in most computational detonation models. This leads to significant discrepancies in detonation cell sizes compared to experimental results. The interaction of gas molecules with shock waves causes the three degrees of freedom—translational, rotational, and vibrational modes—to transition into a state of nonequilibrium, deviating from the Boltzmann distribution typically governing their population at equilibrium. The translational modes of molecules attain equilibrium within a few collisions, while the rotational modes equilibrate after 10 to 20 collisions. In contrast, the vibrational modes require approximately 10^3 to 10^4 collisions to achieve equilibrium. Under detonation conditions, the ignition time scale closely aligns with the vibrational relaxation time scale, necessitating the incorporation of vibrational nonequilibrium effects into the computational models for accurate predictions [1].

Voelkel et al. [2] studied vibrational nonequilibrium effects on hydrogen-air detonation cell structures and found that modeling thermal nonequilibrium increased the mean cell width from 5 mm to 10 mm in 2D simulations. Shi et al. [3] performed thermal nonequilibrium detonation simulations for argon-diluted hydrogen-oxygen mixtures using the space-time conservation element and solution element (CE/SE) method. They examined thermal equilibrium and nonequilibrium cases with and without chemistry-vibration coupling. The chemistry-vibration coupling model provided the closest match to experimental detonation cell widths.

This study utilizes the *hy2Foam* solver, originally designed for simulating reentry hypersonic reacting flows in 11-species air mixtures [4]. Built on the open-source computational platform OpenFOAM, this CFD solver incorporates the Landau-Teller model to simulate vibrational-translational energy exchanges

and employs the Knab model for vibrational-vibrational energy transfer processes. Furthermore, it integrates the Park model, or the coupled vibration-dissociation-vibration (CVDV) framework, to represent chemistry-vibration coupling in the simulations.

This study aims to model the detonation structure and wave propagation in a stoichiometric H₂-O₂ mixture at 10 kPa and 300.15 K using the *hy2Foam* solver. The study explores three approaches: (i) assuming thermal equilibrium for all gas species, (ii) accounting for trans-rotational to vibrational relaxation, and (iii) incorporating both trans-rotational to vibrational relaxation along with the coupled vibration-dissociation-vibration (CVDV) model. The numerical results are compared with the experimental measurements to evaluate the influence of vibrational nonequilibrium on computational modeling.

2 Methodology

In this study, the nonequilibrium Navier-Stokes-Fourier (NSF) equations were utilized to simulate transient compressible reactive flows using *hy2Foam*, a computational framework based on OpenFOAM. Here, N_S denotes the total number of species, and N_m represents the number of molecules constituting the mixture. The numerical formulation of the NSF equations in flux divergence form, expressed in the Cartesian coordinate system is presented in (1).

$$\frac{\partial \mathbf{U}}{\partial t} + \frac{\partial \mathcal{F}}{\partial x_i} = \dot{\mathcal{W}} \quad (1)$$

The conserved vector quantities denoted as \mathbf{U} , are defined as,

$$\mathbf{U} = \{(\rho, \rho_s, \rho u, \rho v, \rho w, E_{ve,m}, E)^T \mid s \in N_S, m \in N_m\} \quad (2)$$

where u, v, w are the components of the velocity vector, ρ is the mass density of the fluid and ρ_s is the partial density of species s . The flux vector \mathcal{F} represents the transport of the conserved quantities within the system. The source term vector $\dot{\mathcal{W}}$ can be written as

$$\dot{\mathcal{W}} = (0, \dot{\omega}_s, 0, 0, 0, \dot{\omega}_{v,m}, 0)^T \quad (3)$$

The term $\dot{\omega}_s$ represents the net mass production rate of species s and $\dot{\omega}_{v,m}$ characterizes the vibrational source terms, which include the vibrational-translational energy exchanges, coupling between chemical reaction rates and vibrational energy modes, as well as vibrational-vibrational energy transfers occurring among interacting species in the system.

The vibrational-translational (V-T) energy transfer is governed by the Landau-Teller equation [5]. This equation describes the V-T energy exchange rate, $Q_{m,V-T}$ and is given in (4).

$$Q_{m,V-T} = \rho_m \frac{\partial e_{ve,m}(T_{ve,m})}{\partial t} = \rho_m \frac{e_{ve,m}(T_{tr}) - e_{ve,m}(T_{ve,m})}{\tau_{m,V-T}}, \quad m \in N_m \quad (4)$$

The specific vibrational energy of molecules $m \in N_m$, denoted as $e_{ve,m}$, relaxes over time based on the relaxation time $\tau_{m,V-T}$. This is determined using the Millikan-White correlation [6], later refined by Park to correct collision cross-section inaccuracies at high temperatures. Due to frequent collisions, translational and rotational energy modes equilibrate quickly and share a single temperature, T_{tr} , while vibrational and other energy modes are characterized by a separate temperature, $T_{ve,m}$.

The governing reaction temperature follows Park's Temperature, defined as $T_P = T_{tr}^\alpha \times T_{ve}^{1-\alpha}$, with $\alpha = 0.7$ for this analysis [4]. Vibrational energy can be gained or lost by molecules m due to chemical

reactions, incorporated via an additional source term in $\dot{\omega}_{v,m}$. Molecular dissociation becomes more likely when vibrational modes are fully excited, a phenomenon effectively modeled by the Coupled Vibration-Dissociation-Vibration (CVDV) framework, originally proposed by Marrone and Treanor [7]. The forward reaction rate k_f is modified as follows:

$$k_f = \frac{Z(T_{tr}) Z(T_{F,m})}{Z(T_{ve,m}) Z(-U_m)} \times A T_{tr}^\beta \exp\left(-\frac{T_a}{T_{tr}}\right) \quad (5)$$

where $U_m = \frac{D_m}{3R_m}$, a factor defined by D_m , the dissociation potential, and R_m , the specific gas constant of the molecules.

$$T_{F,m}^{-1} = T_{ve,m}^{-1} - T_{tr}^{-1} - U_m^{-1} \quad (6)$$

Equation (6) is the modified temperature of the species used in the model and $Z(T)$ denotes the vibrational partition function for the species, truncated by a cutoff N vibrational levels determined from the dissociation potential (D_m) and the characteristic vibrational temperature of the species ($\theta_{v,m}$).

The chemical kinetic mechanism proposed by Burke et al. [8], tailored for high-pressure hydrogen combustion (containing 13 species and 27 reactions), was employed in this study. The original solver, designed for an N₂-O₂ system, utilized equilibrium constants computed from the empirical formulation. In the current work, the thermodynamic data provided by Burke et al. [8] was used to fit the necessary coefficients for the empirical formula using `Cantera` and `Python`.

The present study employs three distinct modeling approaches: (i) assuming all species are in thermal equilibrium, where the single-temperature `hy2Foam` solver is utilized; (ii) incorporating vibrational-translational (V-T) relaxation, where all species are modeled to share a single mixture vibrational temperature T_{ve} , and the two-temperature `hy2Foam` solver is employed along with preferential chemistry-vibration coupling [4], and (iii) extending the V-T relaxation by considering the coupled vibration-dissociation-vibration (CVDV) model.

The computational domain is 350 mm long with a height of 40 mm, and a mesh size of 50 μm is used for computational modeling. Detonation initiation is achieved through a sinusoidal perturbation of a high-enthalpy hotspot to trigger the formation of detonation waves. The numerical discretization employs a central differencing Kurganov scheme with a Van Leer flux limiter for flux evaluation, coupled with the Gauss linear interpolation scheme for spatial gradients.

The experimental investigations were carried out at the Detonation Tube Research Facility of IIT Kanpur. A 3.6 m long linear detonation tube with a 73 mm inner diameter was used. The gas mixture was ignited using a centrally mounted spark plug at the closed end, which also housed ports for a gas feed line, vacuum pump, and pressure gauge to control initial conditions. To promote deflagration-to-detonation transition (DDT), a 300 mm long Shchelkin spiral (8 mm wire diameter, 0.3 blockage ratio) was installed downstream of the spark plug to induce turbulence. The open end was connected to a dump tank via a Mylar diaphragm, which isolated the test mixture until detonation and allowed the safe release of combustion products. Further details on the experimental setup can be found in the literature elsewhere [9].

3 Results and Discussions

To validate the solver, one-dimensional (1D) equilibrium simulations were performed using `hy2Foam` and compared against the predictions from the ZND model. The ZND computations employed the Foundational Fuel Chemistry Model Version 2.0 (FFCM-2), which includes 96 species and 1054 reactions [10], and the Burke mechanism. As shown in Fig. 1, the temperature profiles from `hy2Foam` show

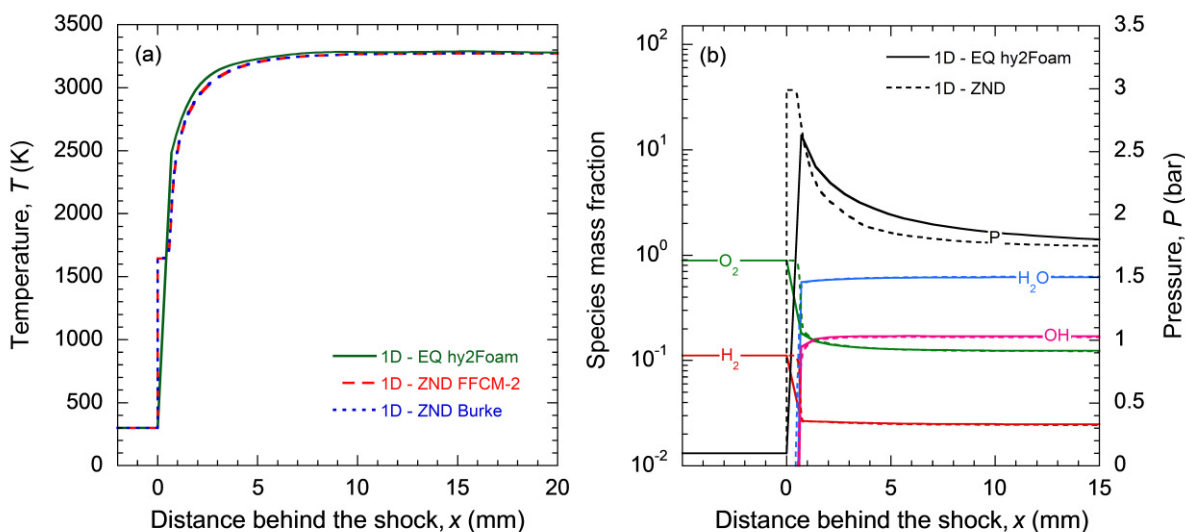


Figure 1: (a) Temperature profiles from 1D equilibrium (EQ) *hy2Foam*, ZND (FFCM-2), and ZND (Burke), (b) Pressure and species profiles from 1D EQ *hy2Foam* (Solid lines) and ZND (FFCM-2) (Dashed lines).

excellent agreement with both FFCM-2 and Burke ZND predictions, demonstrating the solver's capability to accurately capture the thermal structure of the detonation wave. For pressure and species profiles, comparisons were made between *hy2Foam* and ZND simulations using only the FFCM-2 mechanism. The species mass fraction profiles from *hy2Foam* closely coincide with those from the ZND solution, indicating strong agreement in chemical composition evolution. However, the pressure profiles exhibit a slight under-prediction in the peak value in the *hy2Foam* results compared to the ZND model. This discrepancy is attributed to numerical diffusion inherent in the finite volume approach used in *hy2Foam*, whereas the ZND model is idealized and does not account for diffusion. For effective comparison, the 1D *hy2Foam* simulation data was spatially offset so that the detonation front aligns with the origin at $t = 0.25$ ms and propagates from right to left. The detonation front velocity predicted by *hy2Foam* was found to be 0.985 times the Chapman–Jouguet (CJ) speed for both mechanisms, further confirming the solver's consistency across the models.

In computational simulations, the detonation wave was initially overdriven, gradually transitioning to the steady-state Chapman–Jouguet (CJ) condition, allowing for a direct comparison with experimental results. The numerical soot foils are generated by recording peak pressures as detonation waves propagate, revealing significant variations in detonation cell sizes across models. The thermal equilibrium model predicts the smallest average cell size of 2.6 mm (Fig. 2(a)) as the post-shock gas remains in thermal equilibrium. This allows efficient exothermic reactions beyond the induction region, leading to a steady temperature rise. With no energy redistribution, reaction rates remain high, ensuring rapid energy release. Consequently, the reaction zone is more compact, resulting in smaller detonation cell widths than models incorporating nonequilibrium effects.

The V-T relaxation model without CVDV predicts slightly larger detonation cell sizes of 3.8 mm (Fig. 2(b)), reflecting a 47% increase over the thermal equilibrium model. This results from delayed vibrational-translational (V-T) relaxation, where vibrational energy remains elevated post-shock. Consequently, thermal relaxation precedes chemical reactions, temporarily delaying the drop in vibrational temperature and slowing the rise in T_{tr} . Since reaction rates are highly T_{tr} -sensitive, this lag reduces the effective reaction rate and slightly extends the induction length. As a result, detonation cell widths

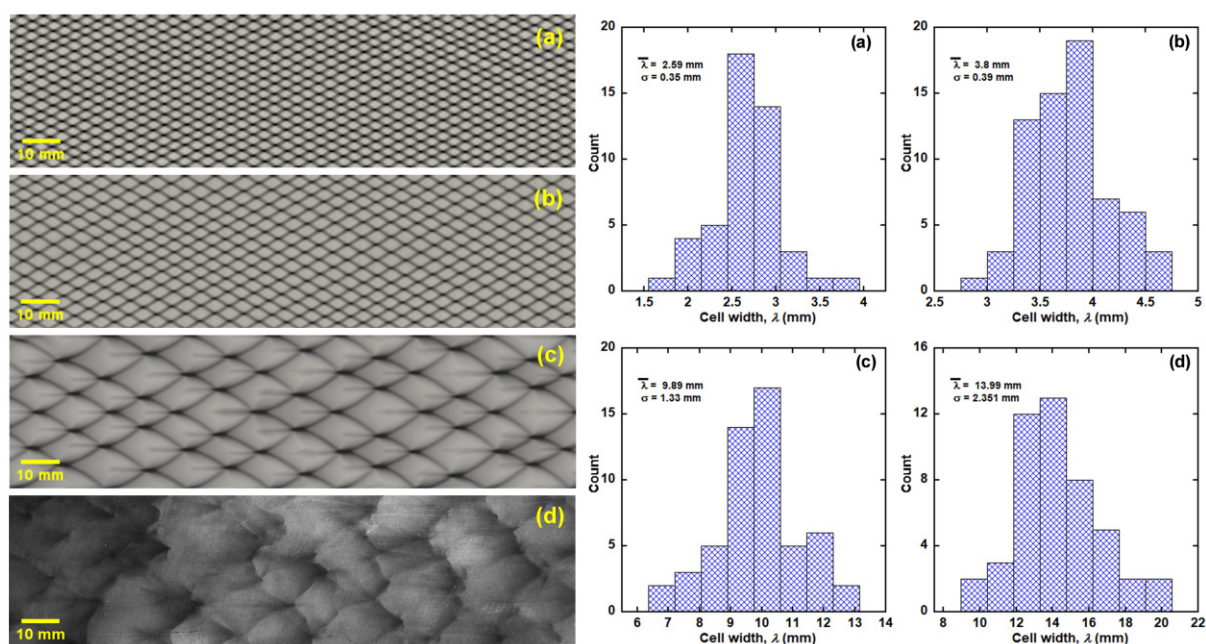


Figure 2: Soot foil and distribution of detonation cell sizes (sample size: 100 cells) in: (a) Thermal equilibrium model, (b) V-T relaxation model without CVDV, (c) V-T relaxation model with CVDV, and (d) Experimental test for a stoichiometric $\text{H}_2\text{-O}_2$ mixture at 10 kPa and 300.15 K.

increase moderately, though the redistribution of vibrational and translational energy eventually allows reaction rates to recover.

When the coupled Vibration-Dissociation-Vibration (CVDV) model is incorporated, the average detonation cell size (Fig. 2(c)) increases significantly to approximately 9.89 mm, which is a factor of 3.3 larger than the thermal equilibrium model and a factor of 2.6 larger than the V-T relaxation model without CVDV. The vibrational nonequilibrium CVDV model accounts for the influence of vibrationally excited molecules, where species in higher vibrational states are more likely to dissociate. This results in a delay in reaction kinetics, as energy that would otherwise contribute to chemical reactions becomes trapped in vibrational modes. Moreover, the interaction between chemical reactions and V-T relaxation plays a crucial role in energy redistribution. As reactions occur, they alter the population of vibrationally excited molecules, affecting the rate at which vibrational energy is transferred to translational and rotational modes. This continuous coupling between chemistry and V-T relaxation prolongs the equilibration process, leading to a sustained delay in energy transfer. As a result, the reaction front weakens, and hence, the delayed energy release and slower thermal equilibration contribute to the formation of larger detonation cell structures in this model.

Experimental soot foil measurements (Fig. 2(d)) show an average detonation cell width of about 14 mm, notably larger than computational predictions. The CVDV-based V-T relaxation model provides the closest match, with a 29% deviation, capturing key vibrational nonequilibrium and dissociation effects. However, it still underestimates the experimental width, likely due to turbulence-chemistry interactions, the absence of vibrational-vibrational energy exchange, and unaccounted 3D effects. In contrast, the V-T relaxation model without CVDV and the thermal equilibrium model predict much smaller cell sizes of 3.8 mm and 2.6 mm, respectively. The thermal equilibrium model assumes rapid energy equilibration, leading to faster reaction kinetics and the smallest cells. The V-T relaxation model without CVDV introduces energy-transfer delays, slightly increasing cell sizes but still underestimating the experimental values. While the present study utilizes the CVDV model, which primarily accounts

for dissociation reactions, a more comprehensive alternative, such as the coupled vibration–chemistry vibration (CVCV) model [2], incorporates additional mechanisms, which include the recombination and exchange reactions. Integrating the CVCV framework in future studies could potentially enhance the fidelity of predictions. Nonetheless, the CVDV-based results show strong agreement with experimental observations, indicating that the key reaction pathways and their nonequilibrium effects are effectively captured within the current modeling approach.

4 Conclusions

The present work highlights the critical role of vibrational nonequilibrium, particularly through the CVDV model, in predicting detonation cell sizes for H₂-O₂ mixtures. The thermal equilibrium model significantly underestimates cell sizes, while the inclusion of vibrational relaxation and dissociation dynamics in the CVDV model produces results that are more consistent with experimental measurements. Furthermore, future research could involve the use of molecular dynamics simulations to refine reaction mechanisms for H₂-O₂ systems at high pressures and temperatures. Additionally, incorporating the effects of molecular diffusion and turbulence into the computational framework could provide a more comprehensive understanding of the detonation structure and improve predictive accuracy for practical applications.

Acknowledgements

The financial support from the Aeronautics Research and Development Board (ARDB) is gratefully acknowledged for the current work (Grant No. ARDB/01/1042000M/I).

References

- [1] Taylor BD, Kessler DA, Gamezo VN, Oran ES. (2013). Numerical simulations of hydrogen detonations with detailed chemical kinetics. *Proceedings of the combustion Institute*, 34(2), 2009-2016.
- [2] Voelkel S, Masselot D, Varghese P L, Raman V. (2016). Analysis of hydrogen-air detonation waves with vibrational nonequilibrium. In *AIP Conference Proceedings* (Vol. 1786, No. 1).
- [3] Shi L, Shen H, Zhang P, Zhang D, Wen C. (2017). Assessment of vibrational non-equilibrium effect on detonation cell size. *Combustion Science and Technology*, 189(5), 841-853.
- [4] Casseau V, Palharini RC, Scanlon TJ, Brown RE. (2016). A two-temperature open-source CFD model for hypersonic reacting flows, part one: zero-dimensional analysis. *Aerospace*, 3(4), 34.
- [5] Landau L. (1936). Theory of sound dispersion. *Physikalische zeitschrift der Sowjetunion*, 10, 34-43.
- [6] Millikan RC, White DR. (1963). Systematics of vibrational relaxation. *The Journal of chemical physics*, 39(12), 3209-3213.
- [7] Treanor CE, Marrone PV. (1962). Effect of dissociation on the rate of vibrational relaxation. *The Physics of Fluids*, 5(9), 1022-1026.
- [8] Burke, MP, Chaos, M, Ju, Y, Dryer, FL, Klippenstein, SJ. (2012). Comprehensive H₂/O₂ kinetic model for high-pressure combustion. *Int. J. Chem. Kinet.*, 44(7), 444–474.
- [9] Singh RK, Dahake A, Yadav CK, Singh AV. (2024). Evaluating the effect of ignition energy on gaseous hydrogen–oxygen detonations. *International Journal of Hydrogen Energy*, 80, 322-331.
- [10] Zhang Y, Dong W, Vandewalle L, Xu R, Smith GP, Wang H. (2023). Foundational Fuel Chemistry Model Version 2.0 (FFCM-2). <https://web.stanford.edu/group/haiwanglab/FFCM2>.